High-Energy MnO_2 Nanowire/Graphene and Graphene Asymmetric Electrochemical Capacitors

Zhong-Shuai Wu,[†] Wencai Ren,[†,*] Da-Wei Wang,[‡] Feng Li,[†] Bilu Liu,[†] and Hui-Ming Cheng[†,*]

[†]Shenyang National Laboratory for Materials Science, Institute of Metal Research, Chinese Academy of Sciences, 72 Wenhua Road, Shenyang 110016, People's Republic of China, and [‡]ARC Centre of Excellence for Functional Nanomaterials, AIBN, The University of Queensland, Brisbane 4072, Australia

ARTICLE

ABSTRACT In order to achieve high energy and power densities, we developed a high-voltage asymmetric electrochemical capacitor (EC) based on graphene as negative electrode and a MnO_2 nanowire/graphene composite (MGC) as positive electrode in a neutral aqueous Na_2SO_4 solution as electrolyte. MGC was prepared by solution-phase assembly of graphene sheets and α-MnO_2 nanowires. Such aqueous electrolyte-based asymmetric ECs can be cycled reversibly in the high-voltage region of 0—2.0 V and exhibit a superior energy density of 30.4 Wh kg^{-1}, which is much higher than those of symmetric ECs based on graphene//graphene (2.8 Wh kg^{-1}) and MGC//MGC (5.2 Wh kg^{-1}). Moreover, they present a high power density (5000 W kg^{-1} at 7.0 Wh kg^{-1}) and acceptable cycling performance of ~79% retention after 1000 cycles. These findings open up the possibility of graphene-based composites for applications in safe aqueous electrolyte-based high-voltage asymmetric ECs with high energy and power densities.

KEYWORDS: graphene · manganese oxide · composite · asymmetric · electrochemical capacitor

High-performance electrochemical energy storage systems are very important for electric vehicles and hybrid electric vehicles.[1−5] Great efforts have been made to develop high-power (10 kW kg^{-1}) electrochemical capacitors (ECs) due to their faster charge and discharge processes, in seconds, than those of batteries.[2] However, ECs suffer from a lower energy density (normally ≤10 Wh kg^{-1}) than batteries.[3] To solve this problem, asymmetric (hybrid) systems have been extensively explored by combining a battery-like Faradic electrode (as energy source) and a capacitive electrode (as power source) to increase the operation voltage, which leads to a notable improvement of the energy density of high-power ECs so that it approaches that of batteries.[6−10]

The keys to achieve high energy and power densities of asymmetric ECs are to use appropriate materials, usually carbon materials, as a capacitive electrode, to design and synthesize suitable materials, especially nanostructured materials, as a Faradic electrode, and to select a suitable electrolyte.[2] Currently, activated carbon (AC) with a high specific surface area and moderate cost is the most widely used material for the capacitive electrode of asymmetric ECs, but capacitance increase is limited because many of the pores in AC are smaller than 0.5 nm and not accessible to hydrate ions (0.6−0.76 nm).[11−14] Previous studies demonstrate that the use of nanostructured redox-active materials (such as MnO_2,[15] Fe_3O_4,[16] NiO[17]) as Faradic electrodes is helpful for an energy density increase at the cost of cyclability. Among them, MnO_2 is one of the most promising materials for low-cost and environment-friendly asymmetric EC devices with high specific capacitance.[18−22] For example, a combination of a carbon capacitive electrode with a MnO_2 pseudocapacitive electrode can lead to a 2 V high-voltage cell in aqueous electrolytes because of the apparent water decomposition overpotential on MnO_2 and the high surface area of carbon.[23,24] Moreover, it has been demonstrated that the use of nanostructured MnO_2/carbon composites as a Faradic electrode can improve the electrical conductivity of the electrode and thus offers the potential for improvement in the cyclability of ECs.[25−27] As far as the electrolytes are concerned, neutral aqueous electrolytes (Na_2SO_4, K_2SO_4) used in ECs have the advantages of high ionic conductivity, low cost, nonflammability, good safety, and convenient assembly in air, compared to organic electrolytes.[23] Also, aqueous-based ECs can deliver much higher power density than organic electrolyte-based ECs due to their high ionic conductivity,[19] and the ability of operating in neutral aqueous electrolyte does not cause environmental problems.

Different from AC, graphene powders, consisting of ultrathin two-dimensional

*Address correspondence to cheng@imr.ac.cn, wcren@imr.ac.cn.

Received for review July 24, 2010 and accepted September 14, 2010.

Published online September 21, 2010.
10.1021/nn101754k

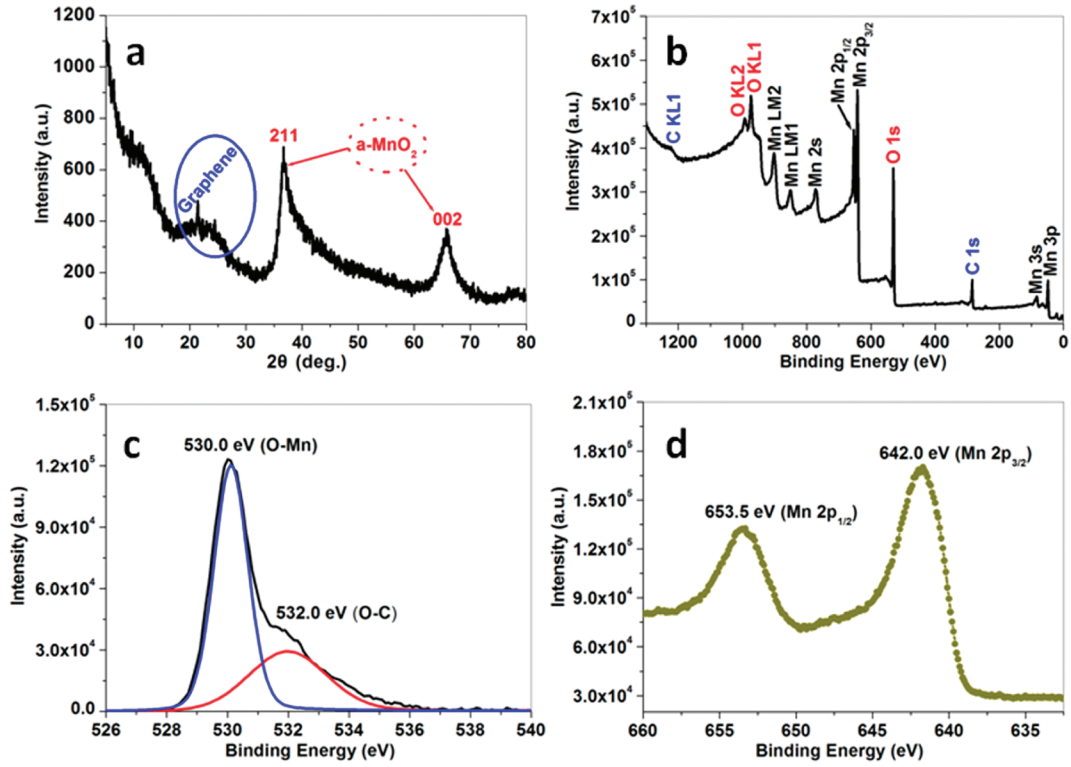

Figure 1. (a) XRD pattern, (b) XPS, (c) O1s XPS, and (d) Mn 2p XPS of MGC. The blue solid ring and red dotted ring in (a) indicate the diffraction peaks of disordered graphene and α-MnO_2, respectively.

(2D) graphene sheets, have a flexible porous structure mainly with mesopores and macropores, in addition to their high electrical conductivity, superior mechanical properties, good electrochemical stability, and high surface area.[28−36] Therefore, graphene is a good candidate for the capacitive electrode since it can provide a large accessible surface area for fast transport of hydrate ions to achieve high double-layer capacitance in aqueous electrolytes.[37,38] In addition, the superior electrical conductivity of graphene makes a nanostructured MnO_2/graphene composite promising for the use as Faradic electrode in asymmetric ECs. More importantly, the presence of nanostructured MnO_2 is able to efficiently prevent the aggregation of graphene sheets caused by van der Waals interactions, consequently leading to an increase in the available electrochemical active surface area and a suitable porous structure for energy storage. Therefore, asymmetric ECs constructed from a nanostructured MnO_2/graphene composite as positive electrode and graphene as negative electrode are expected to exhibit high voltage, high energy, and power densities in neutral aqueous electrolytes.

Here we report the preparation of a MnO_2 nanowire/graphene composite (MGC) by solution-phase assembly of graphene sheets and MnO_2 nanowires and the assembly of asymmetric ECs based on MGC as positive electrode and graphene as negative electrode, which were studied in an aqueous Na_2SO_4 solution. The aqueous electrolyte-based asymmetric EC could be cycled reversibly in a high-voltage region of 0−2.0 V and exhibits a superior energy density of 30.4 Wh kg^{-1}, much higher than those of symmetrical ECs based on graphene//graphene and MGC//MGC and significantly higher than those of other aqueous MnO_2-based asymmetric ECs.[15,23,39−44] Moreover, it has a high power density and reasonable cycling performance.

RESULTS AND DISCUSSION

Figure 1a shows the X-ray diffraction (XRD) pattern of the as-prepared MGC. The low and broad (002) diffraction peak detected at 2θ between 20 and 30° confirms a marginal disordered stacking of graphene sheets, while the other two peaks at 2θ = 37° (211) and 65.7° (002) indexed to α-MnO_2 (JCPDS No.44-0141) are broadened, indicating the poor crystallinity of α-MnO_2 in the composite.[20] Further information on the composition of the as-prepared composite was obtained from X-ray photoelectron spectroscopy (XPS) measurements (Figure 1b). Besides the carbon (C 1s, 284.5 eV) and oxygen (O 1s, 532.0 eV) signals from graphene sheets,[45] the O 1s peak observed at 530.0 eV is assigned to the oxygen bonded with manganese (Mn−O) in α-MnO_2 (Figure 1c).[19] The Mn 2p XPS spectrum exhibits two characteristic peaks at 642.0 and 653.5 eV, corresponding to the Mn $2p_{3/2}$ and Mn $2p_{1/2}$ spin−orbit peaks of α-MnO_2 (Figure 1d), further confirming the presence of α-MnO_2 in the composite.[46] On the basis of the quantitative analysis of XPS data, the atomic percentages of C, O, and Mn in the composite are estimated to be 32.6, 45.7, and 21.7%, respectively,

from which the weight ratio of the MnO_2 component in MGC is estimated to be ~81.5 wt %. It is worth noting that the graphene sheets in the composite have very few residual oxygen-containing functional groups, with a C/O ratio of 14.2 after subtracting the oxygen content bonded in O−Mn of α-MnO_2 in the composite; therefore, a good electrical conductivity is expected.[47,48]

Figure 2 shows scanning electron microscope (SEM) and transmission electron microscope (TEM) images of MGC. It can be seen that the α-MnO_2 component in the composite is MnO_2 nanowires, which are several hundred nanometers to several micrometers in length and homogeneously and densely attached on the surface of graphene sheets (Figure 2a,b and Figure S1 in the Supporting Information). TEM characterization further confirms the intimate contact between the graphene sheets and MnO_2 nanowires with diameters of 10−20 nm (Figure 2c,d and Figure S2). Moreover, high-resolution TEM (HRTEM) shows that the crystallinity of the α-MnO_2 nanowires on the graphene surface is not very high (Figure 2d and Figure S2), consistent with the XRD results. It is believed that, on the one hand, the assembly of nanowires on the surface of graphene sheets to some extent prevents the stacking of graphene sheets due to van der Waals interactions, leading to a large available surface area and rich porous structure for energy storage, while on the other hand, the presence of graphene with high electrical conductivity is favorable to improve the dispersion of MnO_2 nanowires and the electrical conductivity of the composite electrode.

In order to obtain the surface area and porous structure, we measured the liquid nitrogen cryosorption of the as-prepared MGC. The nitrogen adsorption and desorption isotherm shows typical II/IV characteristics (Figure 3a), and its corresponding specific surface area is about 107 $m^2\ g^{-1}$. Moreover, the pores constructed by the graphene sheets and MnO_2 nanowires in MGC are mainly mesoporous structure with a broad pore size distribution of 2−50 nm and an average pore size of ~8.9 nm (Figure 3b). Such a sheet−nanowire structure with high specific surface area and mesopores is favorable for improving both the main pseudocapacitance of α-MnO_2 and the electric double-layer (EDL) capacitance of graphene since the hydrated ions in the electrolyte are easily accessible to the exterior and interior pore surfaces.[11]

To evaluate the electrochemical properties and quantify the specific capacitance of the as-prepared MGC and graphene, we performed cyclic voltammogram (CV) measurements on these two electrode materials in a 1 M Na_2SO_4 aqueous solution using a three-electrode system (Figure 4). The graphene electrode was measured within a potential window of −1.0 to 0.4 V *vs* a saturated calomel electrode (SCE), and MGC was measured within a potential window of 0.0 to 1.0 V *vs* SCE at a scan rate of 10 mV s^{-1}. The CV curve of

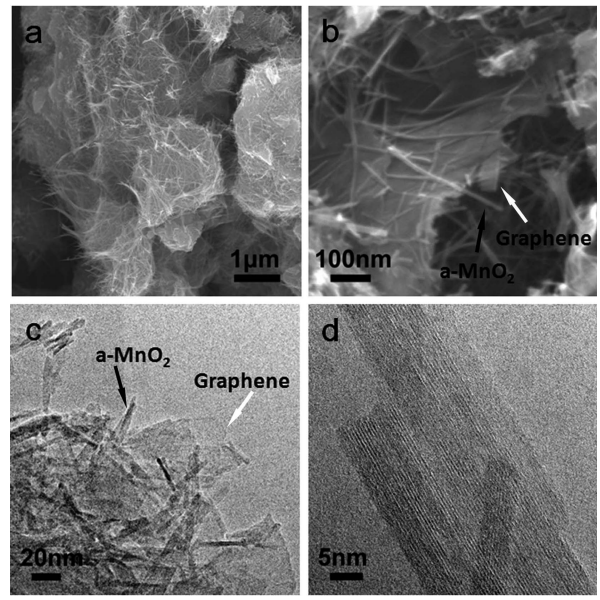

Figure 2. (a) Low-magnification and (b) high-magnification SEM images of MGC, (c) TEM image of MGC, and (d) HRTEM image of the α-MnO_2 nanowires in MGC. The black and white arrows in (b) and (c) indicate the α-MnO_2 nanowires and graphene sheets, respectively.

graphene electrode exhibits a nearly ideal rectangular shape, and no peaks of oxidation and reduction are observed, indicating a typical characteristic of EDL capacitor behavior.[31] The CV shape of the MGC electrode in the potential range of 0.0−1.0 V *vs* SCE is very different from that of the graphene EDL capacitor because the overall capacitance derives from the combined contribution of the main redox pseudocapacitance of MnO_2 and partly from the EDL capacitance of graphene in the composite. Moreover, the CV curve of the MGC electrode exhibits nearly a mirror-image current response on voltage reversal, indicating a good reversibility.[15] On the basis of these results, we can see that the stable voltage window is between 0.0 and 1.0 V for MGC and between −1.0 and 0.4 V for graphene with capacitive behavior, with regard to the SCE. Therefore, it is expected that the operating cell voltage could be extended to about 2 V in mild aqueous solutions if the MGC electrode with a higher cutoff potential (1.0 V) and the graphene electrode with a useful electrochemical window of a lower cutoff potential (−1.0 V) are assembled into asymmetric ECs.

To confirm our hypothesis, we constructed asymmetric ECs by using MGC as the positive electrode and graphene as the negative electrode and using a 1 M Na_2SO_4 solution as electrolyte. Figure 5 shows the schematic of the assembled structure for such asymmetric ECs. To avoid the damage of the cell under high-voltage level during early cycles, it is necessary to polarize each electrode at the same potential and thus to estimate the stable electrochemical windows before cycling the hybrid cell.[49] The CV and galvanostatic charge−discharge measurements were used to evalu-

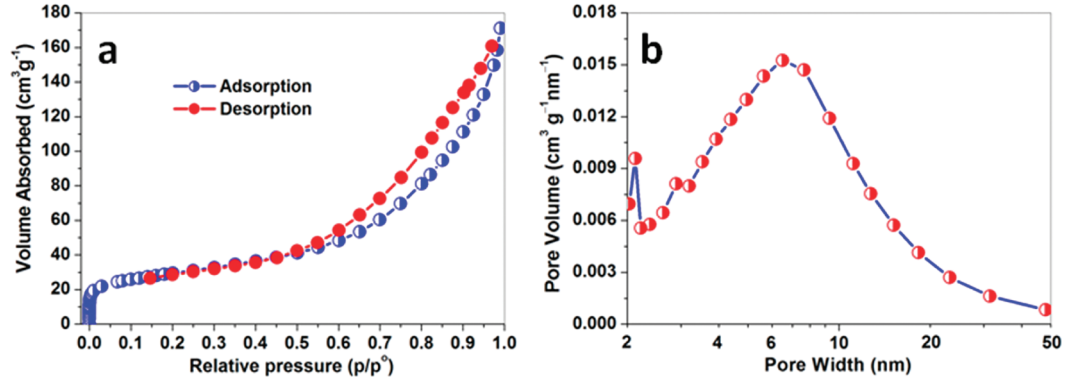

Figure 3. (a) Nitrogen adsorption and desorption isotherm and (b) BJH adsorption pore size distribution of MGC.

ate the stable electrochemical windows of the asymmetric cell. As expected, the results demonstrate that the stable electrochemical windows can be extended to 2.0 V (Figures S3 and S4 in the Supporting Information). The high operating voltage of the asymmetric ECs is due to the perfect combination of the positive and negative stabilities of the two electrodes in different ranges of potentials.[15] Figure 6a shows a typical CV of the asymmetric EC with a voltage of 2.0 V at a scan rate of 10 mV s^{-1}. It is interesting to note that the asymmetric ECs show ideal capacitor behavior with a nearly rectangular CV shape in a neutral aqueous electrolyte. From the charge−discharge curve of the asymmetric ECs (Figure 6b), it can be seen that the potentials of charge−discharge lines are nearly proportional to the charge or discharge time in the Na_2SO_4 electrolyte, indicating a rapid *I*−*V* response. Moreover, the asymmetric EC has acceptable cycling stability performed in the voltage window from 0 to 2 V at a current density of 0.5 A g^{-1} (Figure 6c). A slight capacitance loss is observed after 100 cycles, and the Coulombic efficiency remains above 98%. After 1000 cycles, the asymmetric capacitor retains a high specific capacitance of 24.5 F g^{-1}, about ~79% of the initial capacitance (31.0 F g^{-1}). This cycling performance is comparable to that of some other asymmetric ECs, such as AC//MnO_2 in KOH (20% retention after 1500 cycles) or LiOH electrolyte (more than 80% retention after 1500 cycles),[41] AC//α-$MnO_2 \cdot nH_2O$ (93% retention after 100 cycles),[15] AC//MnO_2 cell without N_2 bubbling (53% retention after 50 000 cycles),[42] AC//Fe_3O_4 (82% retention after 500 cycles),[16] and multiwalled carbon nanotubes (MWCNTs)//MnO_2/MWCNT composite (72.3% retention after 300 cycles).[25] It was assumed that the capacitance fading is due to the corrosion of the current collector caused by the dissolved oxygen in electrolytes together with the excessive positive potential on the MnO_2 electrode[42,44] and/or matching problems.[50,51] We believe that the cycling performance of graphene//MGC asymmetric ECs can be further improved *via* removal of dissolved oxygen in the aqueous electrolyte and optimizing the matching of the mass ratio of positive and negative electrodes, capacitor parameters (such as current and potential matching), volume ratio of the two electrodes, and the ion concentration and pH value of the electrolyte.[50,51]

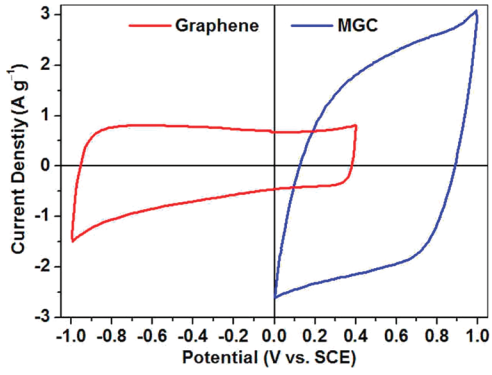

Figure 4. CV curves of graphene and MGC electrodes performed in a three-electrode cell in a 1 M Na_2SO_4 solution at a scan rate of 10 mV s^{-1}.

To further evaluate the electrochemical performance of the graphene//MGC asymmetric ECs, Ragone plot relative to the corresponding energy and power densities was calculated from the galvanostatic capacitance tested in a voltage window of 0−1.5, 0−1.8, and 0−2 V, with current densities of 100 mA g^{-1} to 5 A g^{-1} (Figure 6d). For comparison, we also fabricated two-electrode graphene//graphene and MGC//MGC symmetric ECs, which were tested galvanostatically between 0 and 1.0 V. It is worth noting that the maximum energy density obtained for graphene//MGC asymmetric ECs with a cell voltage of 2.0 V, based on the total mass of active materials, is 30.4 Wh kg^{-1}, which is much higher than those of symmetrical graphene//graphene ECs (2.8 Wh kg^{-1}), MGC//MGC ECs (5.2 Wh kg^{-1}), AC//AC ECs (<10 Wh kg^{-1}),[52] and MnO_2//MnO_2 ECs with 0.6−1.0 V of cell voltage (1.9−3.3 Wh kg^{-1}).[24,39,44] A rough comparison indicates that this value is also significantly higher than those of other MnO_2-based asymmetric ECs with aqueous electrolyte solutions, such as AC//MnO_2 (7.0−28.8 Wh kg^{-1}),[15,23,39−42] AC//$NaMnO_2$ (19.5 Wh kg^{-1}),[43] Fe_3O_4//MnO_2 (8.1 Wh kg^{-1}),[39] polyaniline//MnO_2 (5.86 Wh kg^{-1}),[44] polypyrrole//MnO_2 (7.37 Wh kg^{-1}),[44] and poly(3,4-ethylenedioxythiophene)//MnO_2 (13.5 Wh kg^{-1}).[44] In addition, this assembled asymmetric cell exhibits a good power characteristic of

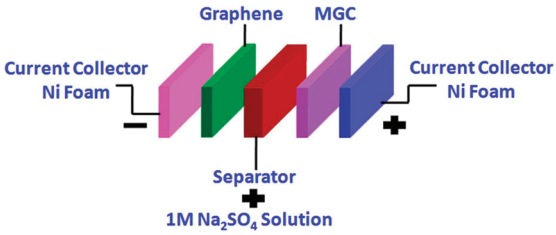

Figure 5. Schematic of the assembled structure of asymmetric ECs based on MGC as positive electrode and graphene as negative electrode.

ECs, and the power density can reach 5000 W kg^{-1} when it keeps a reasonable energy density of 7.0 Wh kg^{-1} in a voltage window of 0−2 V. It should be noted that, to some extent, the applied energy/power densities of the cell can be controlled by selecting a suitable working voltage to satisfy practical requirements (Figure 6d). All of the above results demonstrate that the aqueous graphene//MGC asymmetric ECs can simultaneously achieve high energy density of MGC as appropriate battery-like Faradic electrode and high power density of graphene as suitable capacitor-like electrode. Combined with the other advantages of MnO_2/carbon composites,[18] such as low cost, low toxicity, environmental-friendliness, good safety, and convenient device assembly in air, the aqueous graphene//MGC asymmetric ECs are expected to be a promising energy storage system in electric vehicles and hybrid electric vehicles.

The high-energy electrochemical behavior of graphene//MGC asymmetric ECs can be ascribed to the following factors: (1) The energy density of ECs is proportional to the square of cell voltage; therefore, increasing the cell voltage is an effective way to increase energy density.[53,54] As shown above, compared to the symmetric graphene//graphene (0−1.0 V) and MGC//MGC (0−1.0 V) ECs, the operating cell voltage of graphene//MGC asymmetric ECs is extended to 2 V, consequently resulting in a great increase in energy density. (2) Graphene powders have a flexible porous structure mainly with mesopores and macropores, in addition to their high electrical conductivity, superior mechanical properties, good electrochemical stability, and high surface area.[28−36] This structure provides a large accessible surface area for fast hydrate ion transport, which makes graphene powders superior as capacitive electrode materials to the commercially used AC with limited mesoporous structure. (3) The unique sheet−nanowire structure of MGC (positive electrode) effectively prevents the aggregation of graphene and MnO_2 nanowires and consequently provides a higher specific surface area and richer mesoporous structure, which is favorable for the migration of hydrated ions in the electrolyte to the surfaces of both MnO_2 nanowires

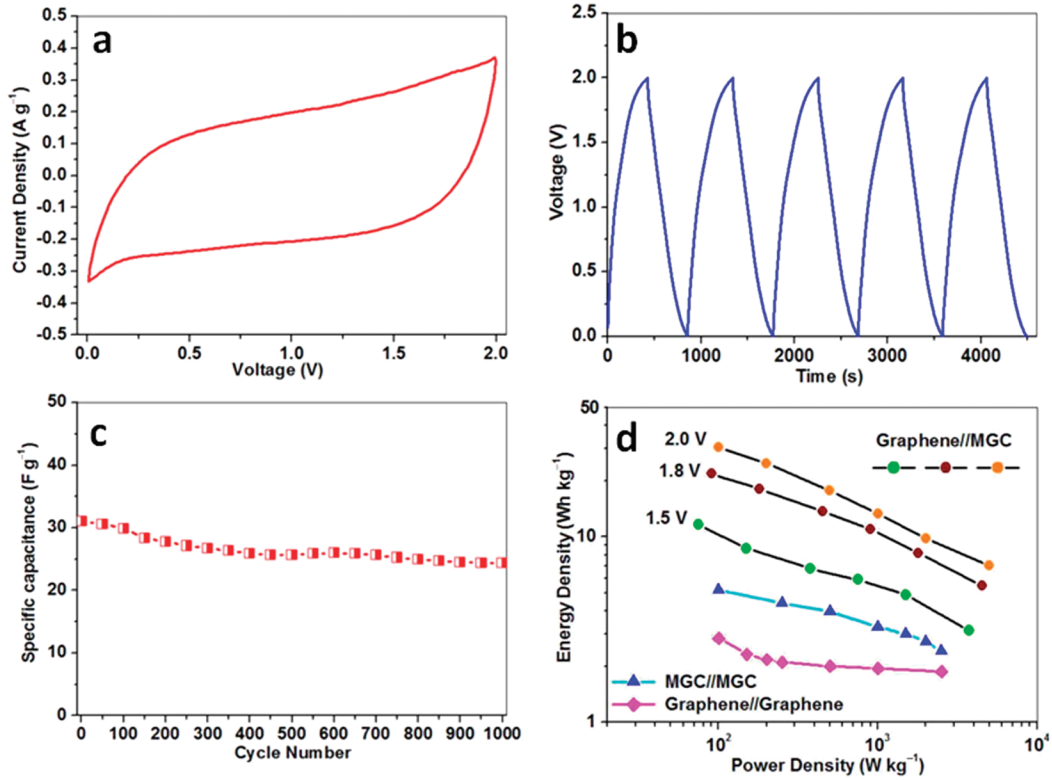

Figure 6. (a) CV curve of the graphene//MGC asymmetric EC with a voltage of 2 V measured at a scan rate of 10 mV s^{-1}. (b) Galvanostatic charge−discharge voltage profile of the graphene//MGC asymmetric EC at a current density of 200 mA g^{-1}. (c) Cycle performance of the graphene//MGC asymmetric EC with a voltage of 2.0 V at a current density of 500 mA g^{-1}. (d) Ragone plot related to energy and power densities of graphene//MGC asymmetric ECs with various voltage windows, graphene//graphene and MGC//MGC symmetric ECs.

and graphene. Furthermore, the excellent electrical conductivity of graphene can significantly decrease the internal resistance of a MGC electrode by the construction of a conductive network. The one-dimensional structure of MnO_2 nanowires with small diameters is also helpful for shortening ion diffusion path, which can greatly reduce the ionic diffusion resistance and charge transfer resistance.[55,56] Therefore, the sheet−nanowire structure of MGC enables high dynamics of charge propagation and short electron transport paths and consequently improves the electrochemical performance of the positive electrode. These findings open new opportunities for graphene and graphene-based composites to develop high-energy electrochemical energy-storage cells by reasonable material design and device construction. We believe that the performance of such devices can be further improved by optimizing the mass (volume) ratio of positive and negative electrodes, the quality and electrical conductivity of graphene, the structure and crystallization of MnO_2, and the graphene content in the MGC positive electrode.

CONCLUSION

We prepared MGC by solution-phase assembly of graphene sheets and α-MnO_2 nanowires and used graphene sheets and MGC as the two electrodes of asymmetric ECs. Asymmetric ECs based on MGC as positive electrode and graphene as negative electrode were assembled and investigated in an aqueous Na_2SO_4 solution. These ECs can be cycled reversibly in the high-voltage region of 0−2.0 V and exhibit an energy density of 30.4 Wh kg^{-1}, which is much higher than those of symmetric ECs based on graphene//graphene (2.8 Wh kg^{-1}) and MGC//MGC (5.2 Wh kg^{-1}) and higher than those of other MnO_2-based asymmetric ECs. Moreover, they have a high energy density of 7.0 Wh kg^{-1} even at a power density of 5000 W kg^{-1} and present an acceptable cycling performance. It is believed that graphene and graphene-based composites have great potential applications in hybrid electric vehicles and electric vehicles where high power and energy storage systems are highly required.

METHODS

Synthesis of MGC. First, chemically derived graphene sheets (with number of layers ≤3) were prepared from natural flake graphite powder (500 mesh) as previously reported,[47] and K-type layered manganese oxide (K_xMnO_2) was synthesized by reduction (Figure S5, Supporting Information).[57,58] Then, the obtained K_xMnO_2 (1 g) was treated with a 0.5 M $NH_4S_2O_8$ solution at 70 °C for 10 h, followed by intercalation and complete exfoliation in a tetrabutylammonium (TBA^+) hydroxide solution (0.35 M) at 70 °C for 10 h to obtain free-standing TBA^+-exfoliated MnO_2 sheets.[59] It is necessary to point out that the colloidal exfoliated MnO_2 sheets are not stable under such hydrothermal flocculation conditions due to the reduced electrostatic interaction between neighboring sheets[60] and thus are spontaneously transformed into α-MnO_2 nanowires (Figure S6). Then, the graphene sheets (50 mg) were added to the above suspension, stirred for 5 h, and then kept at 70 °C for 6 h. Finally, the resulting deposit was filtered, washed several times with deionized water, and dried in a vacuum oven at 70 °C for 12 h to obtain MGC (Figures 1 and 2).

Characterization of MGC. The morphology and microstructure of the as-prepared MGC were characterized by XRD (D-MAX/2400 instrument with Cu Ka radiation between 5 and 80° and an incident wavelength of 0.154056 nm), XPS (ESCALAB 250 instrument with Al Kα radiation), liquid nitrogen cryosorption (Micromeritics, ASAP2010M), SEM (FEI Nova Nano 430 system), and HRTEM (JEOL JEM 2010, 200 kV, and Tecnai F30, 300 kV).

Electrochemical Measurements of MGC and Graphene Electrodes. The MGC used for the positive electrode was prepared by mechanically mixing 70 wt % MGC, 20 wt % acetylene black, and 10 wt % polytetrafluoroethylene (PTFE) binder dispersed in ethanol solvent. Then the mixture was pressed on a Ni-foam grid at a pressure of 6 MPa and dried at 70 °C for 2 h. The graphene negative electrode was prepared by the same procedure with 80 wt % graphene, 10 wt % acetylene black, and 10 wt % PTFE. To construct an asymmetric EC, the loading mass ratio of active materials (MGC/graphene) was estimated to be 7:13 from specific capacitance in term of their CV curves in a three-electrode cell. The cyclic voltammetry test of the individual electrode was performed in a three-electrode cell, in which Ni-foam and a SCE were used as counter electrode and reference electrode, respectively, in a 1 M Na_2SO_4 electrolyte. The cyclic voltammetry and galvanostatic charge−discharge tests of the symmetric ECs (graphene//graphene, MGC//MGC) and the combined asymmetric ECs based on MGC and graphene electrodes separated by a porous nonwoven cloth were performed in a two-electrode cell in the 1 M Na_2SO_4 electrolyte. All of the above electrochemical measurements were carried out by using an electrochemical workstation Solartron 1287.

Acknowledgment. This work was supported by Ministry of Science and Technology of China (No. 2006CB932703), National Science Foundation of China (Nos. 50872136, 50921004, and 50632040), and Chinese Academy of Sciences (No. KJCX2-YW-231).

Supporting Information Available: SEM images of MGC, HR-TEM image of α-MnO_2 nanowires in MGC, the evaluation of the stable electrochemical windows for asymmetric ECs, XRD pattern and SEM images of K-type layered manganese oxide, and the transformation of exfoliated MnO_2 sheets into α-MnO_2 nanowires. This material is available free of charge *via* the Internet at http://pubs.acs.org.

REFERENCES AND NOTES

1. Conway, B. E. *Electrochemical Supercapacitors, Scientific Fundamentals and Technological Applications*; Kluwer Academic/Plenum Press: New York, 1999.
2. Simon, P.; Gogotsi, Y. Materials for Electrochemical Capacitors. *Nat. Mater.* **2008**, *7*, 845–854.
3. Liu, C.; Li, F.; Ma, L. P.; Cheng, H. M. Advanced Materials for Energy Storage. *Adv. Mater.* **2010**, *22*, E28–E62.
4. Su, D. S.; Schlögl, R. Nanostructured Carbon and Carbon Nanocomposites for Electrochemical Energy Storage Applications. *ChemSusChem* **2010**, *3*, 136–168.
5. Zhang, L. L.; Zhao, X. S. Carbon-Based Materials as Supercapacitor Electrodes. *Chem. Soc. Rev.* **2009**, *38*, 2520–2531.
6. Yoshino, A. Hybrid (Asymmetric) Capacitor. *Electrochemistry* **2004**, *72*, 716–719.
7. Wang, Y. G.; Wang, Z. D.; Xia, Y. Y. An Asymmetric Supercapacitor Using RuO_2/TiO_2 Nanotube Composite and Activated Carbon Electrodes. *Electrochim. Acta* **2005**, *50*, 5641–5646.
8. Qu, Q. T.; Shi, Y.; Li, L. L.; Guo, W. L.; Wu, Y. P.; Zhang, H. P.;

Guan, S. Y.; Holze, R. $V_2O_5 \cdot 0.6H_2O$ Nanoribbons as Cathode Material for Asymmetric Supercapacitor in K_2SO_4 Solution. *Electrochem. Commun.* **2009**, *11*, 1325–1328.
9. Hu, X.; Huai, Y.; Lin, Z.; Suo, J.; Deng, Z. A ($LiFePO_4$-AC)/$Li_4Ti_5O_{12}$ Hybrid Battery Capacitor. *J. Electrochem. Soc.* **2007**, *154*, A1026–A1030.
10. Wang, D. W.; Fang, H. T.; Li, F.; Chen, Z. G.; Zhong, Q. S.; Lu, G. Q.; Cheng, H. M. Aligned Titania Nanotubes as an Intercalation Anode Material for Hybrid Electrochemical Energy Storage. *Adv. Funct. Mater.* **2008**, *18*, 3787–3793.
11. Kong, L. B.; Liu, M.; Lang, J. W.; Luo, Y. C.; Kang, L. Asymmetric Supercapacitor Based on Loose-Packed Cobalt Hydroxide Nanoflake Materials and Activated Carbon. *J. Electrochem. Soc.* **2009**, *156*, A1000–A1004.
12. Qu, D. Y. Studies of the Activated Carbons Used in Double-Layer Supercapacitors. *J. Power Sources* **2002**, *109*, 403–411.
13. Largeot, C.; Portet, C.; Chmiola, J.; Taberna, P. L.; Gogotsi, Y.; Simon, P. Relation between the Ion Size and Pore Size for an Electric Double-Layer Capacitor. *J. Am. Chem. Soc.* **2008**, *130*, 2730–2731.
14. Hulicova-Jurcakova, D.; Seredych, M.; Lu, G. Q.; Bandosz, T. J. Combined Effect of Nitrogen- and Oxygen-Containing Functional Groups of Microporous Activated Carbon on Its Electrochemical Performance in Supercapacitors. *Adv. Funct. Mater.* **2009**, *19*, 438–447.
15. Hong, M. S.; Lee, S. H.; Kim, S. W. Use of KCl Aqueous Electrolyte for 2 V Manganese Oxide/Activated Carbon Hybrid Capacitor. *Electrochem. Solid State Lett.* **2002**, *5*, A227–A230.
16. Du, X.; Wang, C. Y.; Chen, M. M.; Jiao, Y.; Wang, J. Electrochemical Performances of Nanoparticle Fe_3O_4/Activated Carbon Supercapacitor Using KOH Electrolyte Solution. *J. Phys. Chem. C* **2009**, *113*, 2643–2646.
17. Wang, D. W.; Li, F.; Cheng, H. M. Hierarchical Porous Nickel Oxide and Carbon as Electrode Materials for Asymmetric Supercapacitor. *J. Power Sources* **2008**, *185*, 1563–1568.
18. Bélanger, D.; Brousse, T.; Long, J. W. Manganese Oxides: Battery Materials Make the Leap to Electrochemical Capacitors. *Electrochem. Soc. Interfaces* **2008**, *17*, 49–52.
19. Qu, Q. T.; Zhang, P.; Wang, B.; Chen, Y. H.; Tian, S.; Wu, Y. P.; Holze, R. Electrochemical Performance of MnO_2 Nanorods in Neutral Aqueous Electrolytes as a Cathode for Asymmetric Supercapacitors. *J. Phys. Chem. C* **2009**, *113*, 14020–14027.
20. Xu, C. J.; Li, B. H.; Du, H. D.; Kang, F. Y.; Zeng, Y. Q. Supercapacitive Studies on Amorphous MnO_2 in Mild Solutions. *J. Power Sources* **2008**, *184*, 691–694.
21. Xu, C. J.; Du, H. D.; Li, B. H.; Kang, F. Y.; Zeng, Y. Q. Capacitive Behavior and Charge Storage Mechanism of Manganese Dioxide in Aqueous Solution Containing Bivalent Cations. *J. Electrochem. Soc.* **2009**, *156*, A73–A78.
22. Brousse, T.; Toupin, M.; Dugas, R.; Athouel, L.; Crosnier, O.; Belanger, D. Crystalline MnO_2 as Possible Alternatives to Amorphous Compounds in Electrochemical Supercapacitors. *J. Electrochem. Soc.* **2006**, *153*, A2171–A2180.
23. Xu, C. J.; Du, H. D.; Li, B. H.; Kang, F. Y.; Zeng, Y. Q. Asymmetric Activated Carbon−Manganese Dioxide Capacitors in Mild Aqueous Electrolytes Containing Alkaline-Earth Cations. *J. Electrochem. Soc.* **2009**, *156*, A435–A441.
24. Khomenko, V.; Raymundo-Pinero, E.; Beguin, F. Optimisation of an Asymmetric Manganese Oxide/Activated Carbon Capacitor Working at 2 V in Aqueous Medium. *J. Power Sources* **2006**, *153*, 183–190.
25. Wang, G. X.; Zhang, B. L.; Yu, Z. L.; Qu, M. Z. Manganese Oxide/MWNTs Composite Electrodes for Supercapacitors. *Solid State Ionics* **2005**, *176*, 1169–1174.
26. Chang, J. K.; Lin, C. T.; Tsai, W. T. Manganese Oxide/Carbon Composite Electrodes for Electrochemical Capacitors. *Electrochem. Commun.* **2004**, *6*, 666–671.
27. Chen, S.; Zhu, J. W.; Wu, X. D.; Han, Q. F.; Wang, X. Graphene Oxide−MnO_2 Nanocomposites for Supercapacitors. *ACS Nano* **2010**, *4*, 2822–2830.
28. Novoselov, K. S.; Geim, A. K.; Morozov, S. V.; Jiang, D.; Zhang, Y.; Dubonos, S. V.; Grigorieva, I. V.; Firsov, A. A. Electric Field Effect in Atomically Thin Carbon Films. *Science* **2004**, *306*, 666–669.
29. Geim, A. K.; Novoselov, K. S. The Rise of Graphene. *Nat. Mater.* **2007**, *6*, 183–191.
30. Geim, A. K. Graphene: Status and Prospects. *Science* **2009**, *324*, 1530–1534.
31. Stoller, M. D.; Park, S.; Zhu, Y.; An, J.; Ruoff, R. S. Graphene-Based Ultracapacitors. *Nano Lett.* **2008**, *8*, 3498–3502.
32. Wang, Y.; Shi, Z. Q.; Huang, Y.; Ma, Y. F.; Wang, C. Y.; Chen, M. M.; Chen, Y. S. Supercapacitor Devices Based on Graphene Materials. *J. Phys. Chem. C* **2009**, *113*, 13103–13107.
33. Wu, Z. S.; Ren, W. C.; Gao, L. B.; Zhao, J. P.; Chen, Z. P.; Liu, B. L.; Tang, D. M.; Yu, B.; Jiang, C. B.; Cheng, H. M. Synthesis of Graphene Sheets with High Electrical Conductivity and Good Thermal Stability by Hydrogen Arc Discharge Exfoliation. *ACS Nano* **2009**, *3*, 411–417.
34. Wang, D. W.; Li, F.; Zhao, J.; Ren, W.; Chen, Z. G.; Tan, J.; Wu, Z. S.; Gentle, I.; Lu, G. Q.; Cheng, H. M. Fabrication of Graphene/Polyaniline Composite Paper *via In Situ* Anodic Electropolymerization for High-Performance Flexible Electrode. *ACS Nano* **2009**, *3*, 1745–1752.
35. Wang, D. W.; Li, F.; Wu, Z. S.; Ren, W.; Cheng, H. M. Electrochemical Interfacial Capacitance in Multilayer Graphene Sheets: Dependence on Number of Stacking Layers. *Electrochem. Commun.* **2009**, *11*, 1729–1732.
36. Tang, L. H.; Wang, Y.; Li, Y. M.; Feng, H. B.; Lu, J.; Li, J. H. Preparation, Structure, and Electrochemical Properties of Reduced Graphene Sheet Films. *Adv. Funct. Mater.* **2009**, *19*, 2782–2789.
37. Lv, W.; Tang, D. M.; He, Y. B.; You, C. H.; Shi, Z. Q.; Chen, X. C.; Chen, C. M.; Hou, P. X.; Liu, C.; Yang, Q. H. Low-Temperature Exfoliated Graphenes: Vacuum-Promoted Exfoliation and Electrochemical Energy Storage. *ACS Nano* **2009**, *3*, 3730–3736.
38. Zhang, L. L.; Zhou, R.; Zhao, X. S. Graphene-Based Materials as Supercapacitor Electrodes. *J. Mater. Chem.* **2010**, *20*, 5983–5992.
39. Cottineau, T.; Toupin, M.; Delahaye, T.; Brousse, T.; Belanger, D. Nanostructured Transition Metal Oxides for Aqueous Hybrid Electrochemical Supercapacitors. *Appl. Phys. A* **2006**, *82*, 599–606.
40. Brousse, T.; Toupin, M.; Belanger, D. A Hybrid Activated Carbon−Manganese Dioxide Capacitor Using a Mild Aqueous Electrolyte. *J. Electrochem. Soc.* **2004**, *151*, A614–A622.
41. Yuan, A. B.; Zhang, Q. L. A Novel Hybrid Manganese Dioxide/Activated Carbon Supercapacitor Using Lithium Hydroxide Electrolyte. *Electrochem. Commun.* **2006**, *8*, 1173–1178.
42. Brousse, T.; Taberna, P. L.; Crosnier, O.; Dugas, R.; Guillemet, P.; Scudeller, Y.; Zhou, Y.; Favier, F.; Belanger, D.; Simon, P. Long-Term Cycling Behavior of Asymmetric Activated Carbon/MnO_2 Aqueous Electrochemical Supercapacitor. *J. Power Sources* **2007**, *173*, 633–641.
43. Qu, Q. T.; Shi, Y.; Tian, S.; Chen, Y. H.; Wu, Y. P.; Holze, R. A New Cheap Asymmetric Aqueous Supercapacitor: Activated Carbon//$NaMnO_2$. *J. Power Sources* **2009**, *194*, 1222–1225.
44. Khomenko, V.; Raymundo-Pinero, E.; Frackowiak, E.; Beguin, F. High-Voltage Asymmetric Supercapacitors Operating in Aqueous Electrolyte. *Appl. Phys. A* **2006**, *82*, 567–573.
45. Schniepp, H. C.; Li, J. L.; McAllister, M. J.; Sai, H.; Herrera-Alonso, M.; Adamson, D. H.; Prud'homme, R. K.; Car, R.; Saville, D. A.; Aksay, I. A. Functionalized Single Graphene Sheets Derived from Splitting Graphite Oxide. *J. Phys. Chem. B* **2006**, *110*, 8535–8539.
46. Li, B. X.; Rong, G. X.; Xie, Y.; Huang, L. F.; Feng, C. Q. Low-Temperature Synthesis of α-MnO_2 Hollow Urchins and

Their Application in Rechargeable Li^+ Batteries. *Inorg. Chem.* **2006**, *45*, 6404–6410.
47. Wu, Z. S.; Ren, W.; Gao, L.; Liu, B.; Jiang, C.; Cheng, H. M. Synthesis of High-Quality Graphene with a Pre-determined Number of Layers. *Carbon* **2009**, *47*, 493–499.
48. Wu, Z. S.; Ren, W.; Wen, L.; Gao, L.; Zhao, J.; Chen, Z.; Zhou, G.; Li, F.; Cheng, H. M. Graphene Anchored with Co_3O_4 Nanoparticles as Anode of Lithium Ion Batteries with Enhanced Reversible Capacity and Cyclic Performance. *ACS Nano* **2010**, *4*, 3187–3194.
49. Lang, J. W.; Kong, L. B.; Liu, M.; Luo, Y. C.; Kang, L. Asymmetric Supercapacitors Based on Stabilized α-$Ni(OH)_2$ and Activated Carbon. *J. Solid State Electrochem.* **2010**, *14*, 1533–1539.
50. Li, J. L.; Gao, F. Analysis of Electrodes Matching for Asymmetric Electrochemical Capacitor. *J. Power Sources* **2009**, *194*, 1184–1193.
51. Zheng, J. P. The Limitations of Energy Density of Battery/Double-Layer Capacitor Asymmetric Cells. *J. Electrochem. Soc.* **2003**, *150*, A484–A492.
52. Wang, D. W.; Li, F.; Liu, M.; Lu, G. Q.; Cheng, H. M. 3D Aperiodic Hierarchical Porous Graphitic Carbon Material for High-Rate Electrochemical Capacitive Energy Storage. *Angew. Chem., Int. Ed.* **2008**, *47*, 373–376.
53. Frackowiak, E.; Beguin, F. Carbon Materials for the Electrochemical Storage of Energy in Capacitors. *Carbon* **2001**, *39*, 937–950.
54. Kotz, R.; Carlen, M. Principles and Applications of Electrochemical Capacitors. *Electrochim. Acta* **2000**, *45*, 2483–2498.
55. Wang, X. Y.; Wang, X. Y.; Huang, W. G.; Sebastian, P. J.; Gamboa, S. Sol−Gel Template Synthesis of Highly Ordered MnO_2 Nanowire Arrays. *J. Power Sources* **2005**, *140*, 211–215.
56. Xu, C. L.; Zhao, Y. Q.; Yang, G. W.; Li, F. S.; Li, H. L. Mesoporous Nanowire Array Architecture of Manganese Dioxide for Electrochemical Capacitor Applications. *Chem. Commun.* **2009**, 7575–7577.
57. Ma, Y.; Luo, J.; Suib, S. L. Syntheses of Birnessites Using Alcohols as Reducing Reagents: Effects of Synthesis Parameters on the Formation of Birnessites. *Chem. Mater.* **1999**, *11*, 1972–1979.
58. Gao, Q. M.; Giraldo, O.; Tong, W.; Suib, S. L. Preparation of Nanometer-Sized Manganese Oxides by Intercalation of Organic Ammonium Ions in Synthetic Birnessite OL-1. *Chem. Mater.* **2001**, *13*, 778–786.
59. Liu, Z.; Ooi, K.; Kanoh, H.; Tang, W.; Tomida, T. Swelling and Delamination Behaviors of Birnessite-Type Manganese Oxide by Intercalation of Tetraalkylammonium Ions. *Langmuir* **2000**, *16*, 4154–4164.
60. Ma, R.; Bando, Y.; Sasaki, T. Directly Rolling Nanosheets into Nanotubes. *J. Phys. Chem. B* **2004**, *108*, 2115–2119.